ARTHRITIS & RHEUMATISM
Vol. 63, No. 6, June 2011, pp 1707–1717
DOI 10.1002/art.30312

Canonical Wnt Signaling Induces Skin Fibrosis and Subcutaneous Lipoatrophy

A Novel Mouse Model for Scleroderma?

Jun Wei,[1] Denisa Melichian,[1] Kazuhiro Komura,[1] Monique Hinchcliff,[1] Anna P. Lam,[1] Robert Lafyatis,[2] Cara J. Gottardi,[1] Ormond A. MacDougald,[3] and John Varga[1]

Objective. **Because aberrant Wnt signaling has been linked with systemic sclerosis (SSc) and pulmonary fibrosis, we sought to investigate the effect of Wnt-10b on skin homeostasis and differentiation in transgenic mice and in explanted mesenchymal cells.**

Methods. **The expression of Wnt-10b in patients with SSc and in a mouse model of fibrosis was investigated. The skin phenotype and biochemical characteristics of Wnt-10b–transgenic mice were evaluated. The in vitro effects of ectopic Wnt-10b were examined in explanted skin fibroblasts and preadipocytes.**

Results. **The expression of Wnt-10b was increased in lesional skin biopsy specimens from patients with SSc and in those obtained from mice with bleomycin-induced fibrosis. Transgenic mice expressing Wnt-10b showed progressive loss of subcutaneous adipose tissue accompanied by dermal fibrosis, increased collagen deposition, fibroblast activation, and myofibroblast accumulation. Wnt activity correlated with collagen gene expression in these biopsy specimens. Explanted skin fibroblasts from transgenic mice demonstrated persistent Wnt/β-catenin signaling and elevated collagen and α-smooth muscle actin gene expression. Wnt-10b infection of normal fibroblasts and preadipocytes resulted in blockade of adipogenesis and transforming growth factor β (TGFβ)–independent up-regulation of fibrotic gene expression.**

Conclusion. **SSc is associated with increased Wnt-10b expression in the skin. Ectopic Wnt-10b causes loss of subcutaneous adipose tissue and TGFβ-independent dermal fibrosis in transgenic mice. These findings suggest that Wnt-10b switches differentiation of mesenchymal cells toward myofibroblasts by inducing a fibrogenic transcriptional program while suppressing adipogenesis. Wnt-10b–transgenic mice represent a novel animal model for investigating Wnt signaling in the setting of fibrosis.**

Systemic sclerosis (SSc) is characterized by inflammation, autoimmunity, small-vessel vasculopathy, and fibrosis in the skin, lungs, and other target organs (1). Fibrosis is attributable to excessive synthesis and deposition of collagens and other extracellular matrix (ECM) molecules, accompanied by accumulation of myofibroblasts positive for α-smooth muscle actin (α-SMA) (2). The source of ECM-producing activated mesenchymal cells is controversial (3,4). In situ transition of resident fibroblasts into myofibroblasts, influx of bone marrow–derived fibrocytes from the circulation, and transdifferentiation of epithelial and endothelial cells into myofibroblasts all might contribute to the expanded pool of biosynthetically active mesenchymal cells. Each of these processes is potently induced by transforming growth factor β (TGFβ) (5).

The pathogenesis of fibrosis in SSc is multifactorial and involves multiple extracellular cues that are important for the initiation or propagation of fibrosis (6). Recent evidence points to the potential importance

Supported by the NIH (grants DK-51563 and DK-62876 to Dr. MacDougald and AR-49025 to Dr. Varga) and the Scleroderma Research Foundation.

[1]Jun Wei, PhD, Denisa Melichian, BA, Kazuhiro Komura, MD, PhD, Monique Hinchcliff, MD, Anna P. Lam, MD, Cara J. Gottardi, PhD, John Varga, MD: Northwestern University Feinberg School of Medicine, Chicago, Illinois; [2]Robert Lafyatis, MD: Boston University School of Medicine, Boston, Massachusetts; [3]Ormond A. MacDougald, PhD: University of Michigan, Ann Arbor.

Address correspondence to John Varga, MD, Section of Rheumatology, Northwestern University Feinberg School of Medicine, 240 East Huron Street, Chicago, IL 60611. E-mail: j-varga@northwestern.edu.

Submitted for publication September 29, 2010; accepted in revised form February 16, 2011.

of Wnt proteins in fibrosis. The Wnt family comprises 19 glycoproteins with dual roles in transcriptional regulation and cell–cell adhesion (7). The paracrine effects of Wnt proteins are mediated via canonical and noncanonical intracellular pathways. Beta-catenin plays a fundamental role in canonical signaling (8). Binding of Wnt ligands to the cell surface receptors Frizzled and low-density lipoprotein receptor–related protein 5 (LRP-5) and LRP-6 results in stabilization and accumulation of β-catenin. In the nucleus, β-catenin regulates target gene expression via the T cell factor family of DNA-binding transcription factors (9). A large number of genes with diverse biologic functions are regulated by β-catenin in a highly cell context–specific manner (10). Transcriptional Wnt targets include Dkk and Axin2 (extracellular and intracellular Wnt inhibitors, respectively), permitting tight regulation of β-catenin signaling via negative feedback.

The Wnt proteins are known primarily as development regulators that are essential for normal embryonic morphogenesis and cell fate determination, including specification of dermal cell identity (11). In the adult, Wnt proteins regulate pluripotent cell differentiation, tissue repair, and regeneration. Acquired defects in Wnt expression or function are associated with cancer, aging, pulmonary arterial hypertension, rheumatoid arthritis, osteosclerosis, and osteoporosis (12–14). A potential role for Wnt proteins in tissue remodeling and pathologic fibrosis is now emerging. Several genes involved in fibrogenesis are directly regulated by Wnt proteins, and pathologic fibrosis has been linked to aberrant Wnt expression and/or activation (15,16). Wnt-10b has potent effects on adipogenesis and osteoblastogenesis (17,18). Transgenic mice in which Wnt-10b is expressed from the fatty acid binding protein 4 (FABP4) promoter showed cold intolerance and resistance to diet-induced obesity (17). Incidentally noted was an increase in dermal thickness, with a reduced number of adipocytes in the skin (17).

There are additional observations linking altered Wnt signaling and cutaneous fibrosis. For instance, TSK-1 mice show aberrant expression of Wnt proteins and their endogenous inhibitors in the skin (19). Moreover, skin biopsy specimens from patients with SSc revealed altered expression of the Wnt signaling axis (20). Skin and lung, the most prominent targets for fibrosis in SSc, express all components of the Wnt pathway, including ligands, receptors, inhibitors, and intracellular signal transducers. Taken together, these observations suggest a plausible role for Wnt signaling in the pathogenesis of fibrosis in patients with SSc.

The results of the current study demonstrate elevated levels of Wnt-10b and evidence of enhanced β-catenin activity in lesional skin biopsy specimens obtained from mice with bleomycin-induced scleroderma and from patients with diffuse cutaneous SSc. In transgenic mice, Wnt-10b overexpression resulted in replacement of subcutaneous adipose tissue with fibrotic tissue. Explanted transgenic fibroblasts showed persistent Wnt-10b elevation and β-catenin signaling in vitro that were associated with fibrotic gene expression and reciprocal suppression of adipogenic genes. In normal fibroblasts and preadipocytes, ectopic Wnt-10b abrogated the induction of adipogenesis and promoted TGFβ-independent fibrogenesis. These results provide compelling evidence for the fibrogenic role of Wnt-10b and suggest that targeting aberrant Wnt-10b expression or activity might be a novel therapeutic strategy for the control of pathologic fibrosis.

MATERIALS AND METHODS

Animals and experimental protocols. FABP4–Wnt-10b–transgenic mice harbor the Wnt-10b gene under the control of a 7.6-kb fragment of the FABP4 promoter/enhancer and show ectopic Wnt-10b expression in both white and brown adipose tissue as well as the bone marrow (17). For this study, transgenic mice were crossed onto an FVB background, and heterozygous female mice were studied at 6 months of age. Each experimental group consisted of 4–6 mice. Animal protocols were institutionally approved by the Northwestern University Animal Care and Use Committee. The expression of Wnt-10b in the skin was examined using a mouse model of bleomycin-induced scleroderma (21). Lesional skin was harvested and analyzed as previously described (21).

To examine Wnt-10b expression in patients with SSc, 4-μm–thick sections were prepared from lesional skin biopsy specimens obtained from 3 patients with diffuse cutaneous SSc and from the forearms of 3 healthy adults and processed for immunohistochemical analysis, using anti-mouse Wnt-10b monoclonal antibodies (1:50 dilution; Santa Cruz Biotechnology) (22). Nonspecific goat IgG served as negative control. The protocol for performing skin biopsies was approved by the Institutional Review Board for Human Studies.

Histochemical analysis. Consecutive 4-μm serial sections of paraffin-embedded skin were stained with hematoxylin and eosin. To evaluate collagen content and organization, deparaffinized sections were stained with Masson's trichrome or picrosirius red and viewed under polarized light (23). Dermal thickness was determined in 5 randomly selected microscopic fields per slide for each mouse (21). Mast cells were identified by astra blue staining (24) and quantified in 6 random microscopic fields per mouse.

Immunohistochemistry, quantitation of tissue collagen, and serum adiponectin assays. Deparaffinized skin sections were treated with target retrieval solution (Dako) and stained with primary antibodies (1:100 dilution) against α-SMA (Sigma) and phosphorylated Smad2 (Cell Signaling

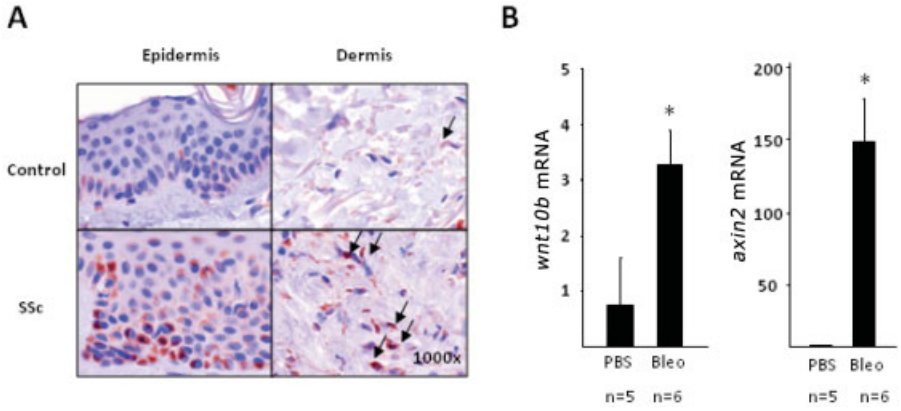

Figure 1. Increased cutaneous Wnt-10b expression and activity in patients with systemic sclerosis (SSc) and in a mouse model of skin fibrosis. **A,** Representative images of lesional skin biopsy specimens obtained from patients with diffuse cutaneous SSc (n = 3) and healthy control subjects (n = 3). Specimens were examined by immunohistochemistry, using antibodies to Wnt-10b. **Arrows** indicate immunopositive cells in the dermis. **B,** Gene expression levels in lesional skin from mice injected with bleomycin (bleo) and control mice injected with phosphate buffered saline (PBS). Total RNA was isolated, and gene expression levels were examined by real-time quantitative polymerase chain reaction. Results were normalized to *36B4*. Bars show the mean ± SD of triplicate determinations. $* = P < 0.05$ versus PBS.

Technology). Bound antibodies were detected using secondary antibodies from the HistoMouse-Max kit (Zymed) and the DakoCytomation EnVision+ System-HRP according to the manufacturers' instructions. Substitution of primary antibody with isotype-matched IgG served as a negative control. Sections were counterstained with hematoxylin and viewed under an Axioskop microscope (Zeiss). Images were captured by the Nuance Multiple Spectra CCD system, using Nuance 2.10 software. Semiquantitative evaluation of immunohistochemical reactions was performed in a blinded manner. The collagen content of the skin was quantified by colorimetric assays (Biocolor). Serum adiponectin levels were determined by enzyme-linked immunosorbent assays (R&D Systems).

RNA isolation and real-time quantitative polymerase chain reaction (qPCR). Total RNA was isolated from skin tissue or explanted fibroblasts or preadipocytes and subjected to qPCR analysis, as previously described (25). Information regarding the primer pairs used for PCR are available from the corresponding author. The results of triplicate determinations are expressed as the fold change in messenger RNA (mRNA) levels relative to control (*36B4*) in each sample.

Cell cultures and differentiation assays. Primary fibroblast cultures were established by explantation from skin biopsy specimens obtained from the interscapular region of transgenic mice and their wild-type (WT) littermates and studied at early confluence (24). Mouse 3T3-L1 preadipocytes (American Type Culture Collection) were seeded in 24-well plates and infected at early confluence with Wnt-10b adenovirus or control green fluorescent protein adenovirus. Cultures were incubated in differentiation medium (DM2-L; Zen-Bio) for 48 hours, followed by adipocyte medium (Zen-Bio) for up to 7 days and stained with oil red O (26). Experiments were repeated at least 3 times. Cellular oil red O uptake was quantitated by dissolving in 2-propanol and measuring the optical density at 510 nm (27). In other experiments, preadipocyte cultures were stained with primary antibodies specific for perilipin (R&D Systems), type I collagen, adiponectin, and Alexa 594–conjugated donkey anti-goat IgG or Alexa 488–conjugated donkey anti-rabbit IgG as secondary antibody. Nuclei were identified using DAPI. Following stringent washing, slides were examined using a Zeiss 510 UV Meta confocal microscope. Each experiment was repeated at least 3 times, with consistent results. Primary cultures of human dermal fibroblasts were established by explantation from neonatal foreskins and studied between passages 4 and 8 (28). Wnt-10b retrovirus infections of confluent fibroblasts were performed as previously described (18). In selected experiments, preadipocytes or fibroblasts were incubated with the selective ALK-5 inhibitor SB431542 (10 μM) for 5 days.

Western blot analysis and inhibitor of β-catenin and T cell factor 4 pull-down assays. Total protein was extracted from skin biopsy specimens or explanted fibroblasts. Aliquots containing equal amounts of proteins (10–15 μg) were subjected to Western blot analysis using primary antibodies to type I collagen (1:400 dilution; Southern Biotechnology), α-SMA (1:5,000; Sigma), FABP4 (1:1,000; BD Biosciences), active β-catenin (1:1,000; Millipore), or GAPDH (1:200; Cell Signaling Technology) (29). Autoradiograms were scanned, and band intensities were determined using ImageJ software. Results were normalized against the intensity of GAPDH in each sample. The cadherin-free signaling pool of β-catenin was quantitated in whole tissue lysates of mouse skin by affinity precipitation with glutathione S-transferase immobilized to glutathione-coupled Sepharose (Sigma) and analyzed by Western blotting, as described previously (30).

Statistical analysis. Results are expressed as the mean ± SD. Student's *t*-test was used for comparisons between 2 groups. *P* values less than 0.05 were considered significant.

RESULTS

Elevated Wnt-10b expression and activity in fibrotic skin. We examined Wnt-10b expression in the skin obtained from patients with SSc. (Information regarding the clinical characteristics of the patients is available from the corresponding author.) Immunohistochemistry revealed only faint expression of Wnt-10b in skin biopsy specimens obtained from healthy control subjects, exclusively in the basal layer of the epidermis. In contrast, Wnt-10b was abundantly expressed in lesional skin biopsy specimens from patients with SSc (Figure 1A). Strong immunoreactivity was seen in epidermal cells as well as in numerous stromal cells within the densely collagenous dermis.

Next, we examined *wnt-10b* expression in the skin of mice with bleomycin-induced scleroderma (31). Female C57BL/6J mice (8–12 weeks of age) were given daily subcutaneous injections of phosphate buffered saline (PBS) or bleomycin for 14 days and were killed on day 28. A >70% increase in dermal thickness was evident in the lesional skin of bleomycin-treated mice, and the subcutaneous adipose layer showed marked atrophy (results not shown). Real-time qPCR analysis showed that the expression of *wnt-10b* mRNA in the lesional skin of bleomycin-injected mice was increased 4-fold compared with that in PBS-treated controls (Figure 1B). Moreover, mRNA levels of *axin2*, a canonical Wnt target gene, were increased ~100-fold (Figure 1B).

Spontaneous dermal fibrosis and adipose tissue loss in Wnt-10b–transgenic mice. Transgenic mice were used to investigate the effect of Wnt-10b. The body weights of FABP4–Wnt-10b–transgenic mice and their WT littermates, all of which were fed a normal chow diet for up to 6 months, did not differ significantly (data not shown). However, a striking loss of visceral fat was evident in the transgenic mice, with markedly reduced epididymal and perirenal adipose tissue. Serum levels of adiponectin, an adipokine produced by adipose tissue,

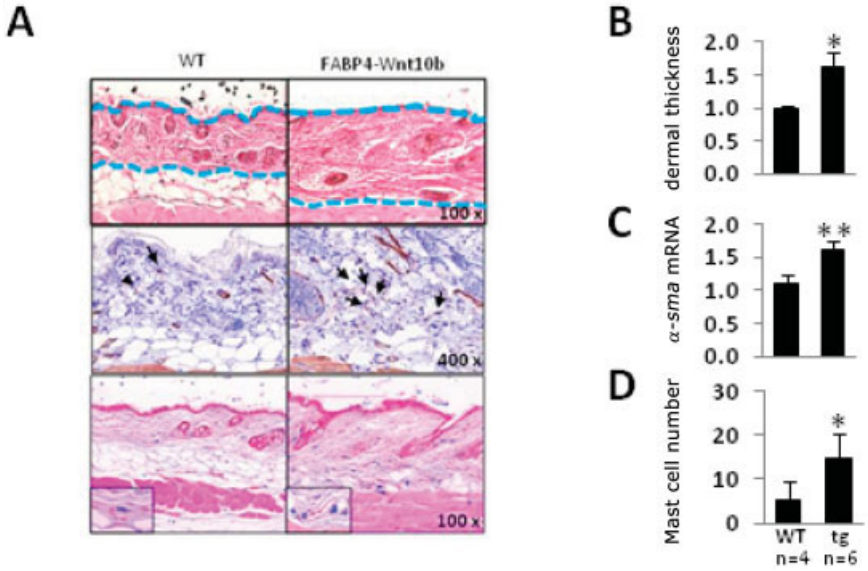

Figure 2. Spontaneous dermal fibrosis and loss of adipose tissue in Wnt-10b–transgenic (tg) mice. **A,** Skin biopsy specimens from 6-month-old wild-type (WT) mice and fatty acid binding protein 4 (FABP4)–Wnt-10b–transgenic mice, showing hematoxylin and eosin staining (top panels), immunohistochemistry with antibodies to α-smooth muscle actin (α-SMA; middle panels), and astra blue staining (lower panels). Boxed areas show high-magnification (× 400) views. Dashed lines indicate the extent of the dermis. **Arrows** indicate α-SMA–positive fibroblasts. **B,** Dermal thickness in WT and transgenic mice. Bars show the mean ± SD of 5 determinations for 4–6 mice in each group. **C,** Expression of *α-sma* mRNA in the skin of WT and transgenic mice, as determined by real-time quantitative polymerase chain reaction. Results were normalized to *36B4* mRNA. Bars show the mean ± SD of triplicate determinations for 3–6 mice in each group. **D,** Number of astra blue–positive cells in the dermis of WT and transgenic mice, as counted in 6 random microscopic fields per mouse. Bars show the mean ± SD. * = $P < 0.05$; ** = $P < 0.005$ versus WT.

were reduced by >80% in transgenic mice compared with WT mice (0.7 μg/ml versus 5.6 μg/ml; $P < 0.005$). Examination of the skin revealed abundant subcutaneous adipose tissue consisting of 2–3 layers of large adipocytes in WT mice, whereas adipocytes in Wnt-10b–transgenic mice were virtually absent from the hypodermis, and adipose tissue was largely replaced by fibrous tissue (Figure 2A, top panels). Although the epidermis appeared to be similar in transgenic and WT mice, the dermal thickness in transgenic mice was increased by >60% (Figure 2B).

The expression of myofibroblasts, which plays a central role in the development and progression of tissue fibrosis, was significantly increased in the dermis of transgenic mice (Figure 2A, middle panels), and the results of qPCR analysis demonstrated a 50% increase in *α-sma* mRNA levels (Figure 2C). Although the thickened dermis showed a general paucity of infiltrating cells, granular cells identified as mast cells by astra blue staining were present in transgenic mice, generally in close proximity to dermal blood vessels (Figure 2A, bottom panels). The number of mast cells in transgenic mice was increased >3-fold compared with the number of mast cells in WT controls (Figure 2D).

Correlation between increased skin collagen accumulation in Wnt-10b–transgenic mice and Wnt activity. Several approaches were taken to evaluate collagen accumulation in the skin. Masson's trichrome and picrosirius red stainings showed markedly increased collagen deposition in the dermis of transgenic mice compared with their WT littermates (Figure 3A). Collagen fibers in the dermis of transgenic mice had a woven architecture distinct from the nearly parallel pattern seen in WT mice and displayed enhanced refraction under polarized light, indicating more mature collagen (32). Prominent collagen accumulation between muscle bundles was seen in transgenic mice but not in their WT littermates. Immunoblot analysis showed 2-fold higher levels of collagen in the dermis of transgenic mice compared with that of WT controls (Figure 3B). The increase in skin collagen was confirmed by Sircol assays (data not shown). In contrast, levels of the adipocyte marker FABP4 were significantly reduced in transgenic mice (Figure 3C).

The levels of *wnt-10b* mRNA in the skin, as determined by qPCR analysis, were ~40-fold higher in transgenic mice compared with their WT littermates (Figure 4A). To determine whether the Wnt-10b in skin was biologically active, the levels of *axin2* mRNA were examined. The results showed a 10-fold increase in *axin2*

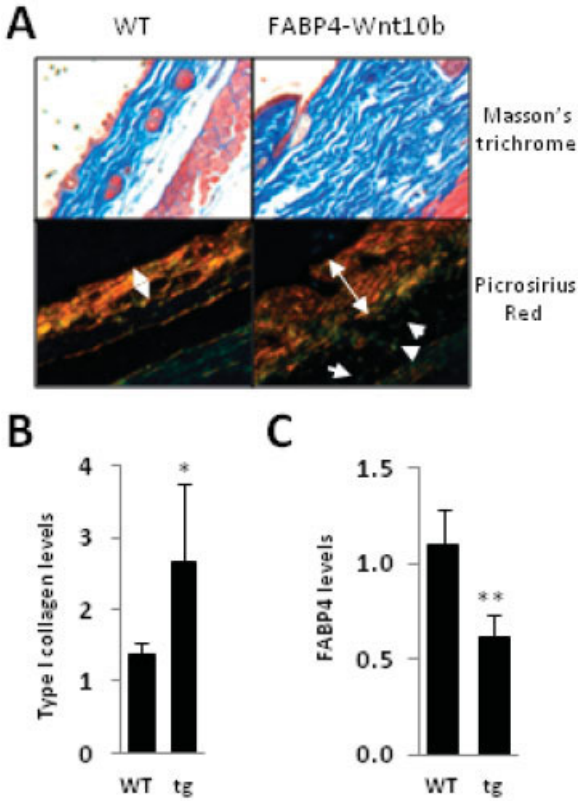

Figure 3. Increased collagen accumulation in the skin of Wnt-10b–transgenic mice. **A,** Representative images of skin biopsy specimens obtained from WT mice and FABP4–Wnt-10b–transgenic mice, showing staining with Masson's trichrome or picrosirius red. **Arrows** indicate collagen bundles within muscle layers. **Double-headed arrows** indicate the dermal border. Original magnification × 200. **B** and **C,** Type I collagen and FABP4 levels, respectively, in the dermis of WT and transgenic mice, as determined by immunoblot analysis and densitometry. Results were normalized to GAPDH. Bars show the mean ± SD of triplicate determinations for 4–6 mice in each group. * = $P < 0.05$; ** = $P < 0.005$ versus WT. See Figure 2 for definitions.

mRNA in Wnt-10b–transgenic mice compared with WT mice. The expression of other markers of canonical Wnt signaling, such as *dkk1*, was also significantly elevated in transgenic mice. Moreover, as shown in Figure 4B, transgenic mice had elevated levels of activated β-catenin in the skin compared with WT control mice. Profibrotic gene expression (*col1a1*, *col1a2*, and *ctgf*) was 3–7-fold increased in skin from Wnt-10b–transgenic mice compared with WT mice (Figure 4C). The increased levels of *col1a1* mRNA were strongly correlated with *axin2* mRNA levels in the same tissues (Figure 4D).

In order to determine the role that TGFβ might play in mediating Wnt-10b–associated fibrosis, the in

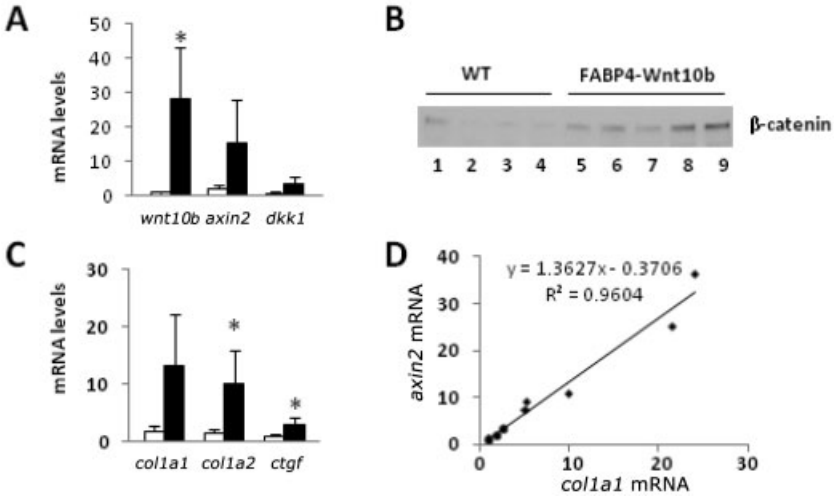

Figure 4. Collagen mRNA expression correlates with elevated *Wnt-10b* expression and activity in the skin. **A** and **C,** Expression of *wnt-10b*, *axin2*, and *dkk1* mRNA (**A**) and of the profibrotic genes *col1a1*, *col1a2*, and *ctgf* (**C**) in the skin of WT mice (open bars) and transgenic mice (solid bars). Results were normalized to *36B4*. Bars show the mean ± SD of triplicate determinations for 3–5 mice in each group. $* = P < 0.05$. **B,** Levels of activated β-catenin in the skin of WT mice and FABP4–Wnt-10b–transgenic mice, as determined by inhibitor of β-catenin and T cell factor 4 pull-down assay. Each lane represents an individual mouse. **D,** Positive correlation between *col1a1* mRNA levels and *axin2* mRNA levels in WT mice (●) and Wnt-10b–transgenic mice (■). See Figure 2 for definitions.

situ expression of phosphorylated Smad2, a highly sensitive and specific marker of TGFβ activity, was assessed. Immunohistochemical analysis showed no significant difference in the numbers of phosphorylated Smad2–positive fibroblasts in the dermis of transgenic mice and WT mice, although the levels of *tgfβ* mRNA were elevated in transgenic mice (data not shown).

Elevated fibrotic gene expression in explanted transgenic fibroblasts. Fibroblasts are the major cell population responsible for ECM production in skin. Because Wnt-10b–transgenic mice showed dermal fibrosis, we questioned whether FABP4-driven Wnt-10b expression was associated with constitutive fibroblast activation. To address this question, primary skin fibroblast cultures were established by explantation from Wnt-10b–transgenic mice and their WT littermates. After 2–3 serial passages, Wnt-10b–transgenic fibroblasts and WT fibroblasts showed comparable morphologic characteristics and proliferation rates (data not shown). Confluent transgenic fibroblasts showed a marked and persistent elevation in *wnt-10b* mRNA levels (Figure 5A). Levels of the canonical Wnt target *axin2* showed a 20-fold increase. *Col1a1* and *col1a2*, *α-sma*, and *ctgf* mRNA (Figure 5B) and protein levels (Figure 5C) were all elevated in explanted Wnt-10b–transgenic fibroblasts. Activation of canonical Wnt signaling in these cells was detected using antibodies to active β-catenin (Figure 5C). At the same time, the expression of the adipogenesis markers *fabp4*, peroxisome proliferator–activated receptor γ1 (*pparγ1*), and *pparγ2* was diminished in transgenic fibroblasts (Figure 5D).

To investigate how Wnt signaling modulates adipogenesis, fibroblasts were incubated with adipocyte differentiation medium. Under these conditions, WT fibroblasts readily underwent adipogenesis in response to DM2. In contrast, fibroblasts explanted from Wnt-10b–transgenic mice were relatively resistant to the adipogenic effects of DM2. Consistent with these observations, real-time qPCR analysis showed that induction of the adipogenic markers *fabp4* and *adiponectin* was reduced in transgenic fibroblasts (data not shown).

Role of ectopic Wnt-10b in adipogenesis and fibrotic responses in vitro. Because dermal fibrosis in transgenic mice was associated with a reciprocal reduction in subcutaneous adipose tissue, we next investigated Wnt-10b–induced regulation of adipogenesis in vitro in 3T3-L1 preadipocytes. In the presence of DM2 adipogenic differentiation medium, 3T3-L1 preadipocytes acquired a rounded shape and accumulated prominent oil red O– and perilipin-positive intracellular lipid droplets

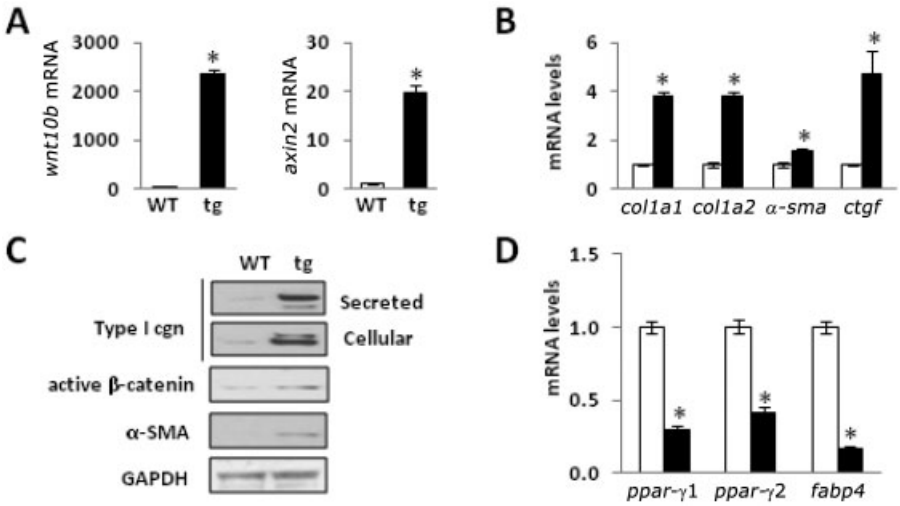

Figure 5. Elevated fibrotic gene expression in explanted Wnt-10b–transgenic mouse fibroblasts in vitro. **A** and **B,** Explanted transgenic (solid bars) and WT (open bars) mouse skin fibroblasts were examined in parallel. RNA was isolated and subjected to real-time quantitative polymerase chain reaction (PCR). Results were normalized to *36B4* mRNA. Bars show the mean ± SD of triplicate determinations in a representative experiment. **C,** Whole cell lysates were examined by immunoblot analysis. **D,** Relative mRNA levels were determined by real-time quantitative PCR. Bars show the mean ± SD. ∗ = $P < 0.05$ versus WT. cgn = collagen (see Figure 2 for other definitions).

(Figure 6A). Ectopic Wnt-10b inhibited adipogenesis, with a >70% reduction in oil red O uptake (data not shown). Real-time qPCR analysis confirmed elevated expression of *wnt-10b* and *axin2* in Wnt-10b–infected cells (Figure 6B). Wnt-10b inhibited expression of the adipogenesis markers *pparγ*, *fabp4*, and *adiponectin* in both unstimulated and DM2-stimulated preadipocytes (Figure 6C, and results not shown). Moreover, Wnt-10b induced the expression of fibrogenic genes in preadipocytes while simultaneously diminishing the expression of adiponectin in the same cells (Figure 6D). Importantly, treatment of the preadipocytes with the ALK-5 inhibitor SB431542, which blocks canonical TGFβ signaling, failed to abrogate the up-regulation of collagen and α-SMA gene expression by Wnt-10b (Figure 6E).

The modulation of fibrogenesis by Wnt-10b was next examined in normal fibroblasts. Confluent foreskin fibroblasts were infected with Wnt-10b for 5 days. Western blot analysis of whole cell lysates showed a marked increase in type I collagen levels in Wnt-10b–expressing fibroblasts (Figure 6F, and results not shown). Incubation with SB431542 failed to abrogate Wnt-10b–induced stimulation of collagen and α-SMA gene expression in human fibroblasts (results not shown). The fibrogenic effects of ectopic Wnt-10b in preadipocytes and dermal fibroblasts therefore appeared to be independent of TGFβ/Smad signaling. Taken together, these results demonstrate that Wnt-10b is sufficient by itself to cause stimulation of fibrogenesis markers and reciprocal repression of adipogenesis in mesenchymal cells.

DISCUSSION

Fibrosis in the skin and internal organs is a major factor contributing to a poor prognosis in SSc. Our studies provide evidence that Wnt-10b is sufficient to induce striking skin fibrosis in transgenic mice associated with replacement of the subcutaneous adipose layers. These changes are similar to the dermatopathologic features of scleroderma, in which progressive disease is associated with replacement of fat by fibrotic tissue and with characteristic tethering of the skin. The expression of collagen and connective tissue growth factor (CTGF) was markedly increased in the skin of Wnt-10b–transgenic mice, whereas the expression of genes involved in regulating adipogenesis was suppressed. These observations point to a reciprocal relationship between adipogenic and fibrogenic gene expression and a crucial role for Wnt-10b/β-catenin signaling in regulating the developmental balance between adipogenesis and fibrogenesis. Transgenic skin fibroblasts displayed elevated Wnt-10b expression and β-catenin signaling that were associated with increased expression of fibrogenesis markers and resistance to the induction of adipogenesis.

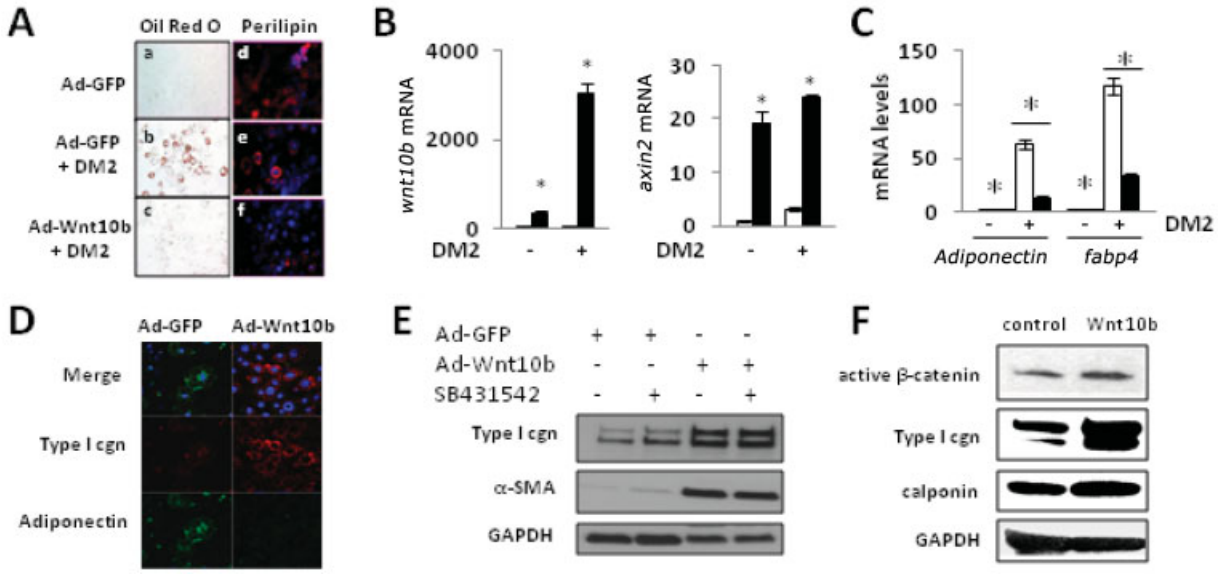

Figure 6. Ectopic Wnt-10b inhibits adipogenesis and induces fibrotic responses. **A–E,** Confluent 3T3-L1 cells were infected with green fluorescent protein adenovirus (AdGFP; open bars in **B** and **C**) or AdWnt-10b (solid bars in **B** and **C**) for 48 hours. Adipogenic differentiation was induced as described in Materials and Methods. **A,** Cultures were fixed after 7 days and stained with oil red O or antiperilipin antibodies (blue indicates staining with DAPI, and red shows staining with perilipin). Original magnification × 200. **B** and **C,** RNA was isolated and examined by real-time quantitative polymerase chain reaction. Results were normalized to *36B4*. Bars show the mean ± SD of triplicate determinations from a representative experiment. $* = P < 0.05$ versus AdGFP. **D,** Representative confocal microscopic images are shown, in which green indicates adiponectin and red shows type I collagen (cgn). Original magnification × 400. **E,** Cultures were infected with AdWnt-10b or AdGFP in the presence or absence of SB431542 (10 μM) for 5 days, and whole cell lysates were subjected to immunoblot analysis. **F,** Foreskin fibroblasts were infected with Wnt-10b retrovirus or empty retrovirus for 5 days, and whole cell lysates were subjected to immunoblot analysis. See Figure 2 for other definitions.

In mesenchymal cells, ectopic Wnt-10b induced collagen gene expression while abrogating adipogenesis. These observations suggest that Wnt-10b induces β-catenin signaling in cutaneous mesenchymal cells, leading to sustained fibrotic responses.

Transgenic mice expressing Wnt-10b are viable and appear healthy, implying that despite the inhibitory effects of Wnt-10b on adipocyte differentiation, neonatal adipogenesis is unaffected in these mice (31). This may indicate that the FABP4 promoter is turned on at a later stage during development. We observed no significant differences in weight between WT and transgenic mice at 6 months of age, despite the substantial reduction in both subcutaneous and visceral fat deposits, possibly reflecting a concomitant 33% increase in skin thickness and weight. Moreover, Wnt-10b–transgenic mice show increased osteoblastogenesis and bone formation and have increased bone mass (18). Dermal thickening was associated with marked accumulation of collagen and increased expression of type I collagen genes. Multiple lines of evidence indicate that the fibrogenic effects of Wnt-10b are not mediated through endogenous TGFβ. The extent of Smad2 phosphorylation in lesional skin was comparable in WT and transgenic mice, even though *tgfb1* mRNA levels were elevated in transgenic mice. Importantly, ectopic Wnt-10b had no effect of Smad2/3 phosphorylation or TGFβ production in explanted lesional fibroblasts. Moreover, fibrotic responses induced by ectopic Wnt-10b in preadipocytes and fibroblasts were not abrogated by blocking TGFβ/Smad signaling using an ALK-5 inhibitor.

Explanted transgenic skin fibroblasts showed persistent Wnt-10b expression and β-catenin signaling in vitro. Constitutive β-catenin signaling was associated with elevated collagen gene expression and a reciprocal decrease in expression of the adipogenic master regulator PPARγ and its target gene FABP4. The expression of PPARγ is known to be suppressed by Wnt-10b in a variety of cell types (18,33). Multipotent mesenchymal progenitor cells differentiate into a variety of cell types, including adipocytes and fibroblasts. PPARγ plays a crucial role in the lineage specification of mesenchymal progenitor cells (34), and its suppression by canonical Wnt proteins inhibits adipogenesis while promoting osteoblastic differentiation of mesenchymal progenitor cells (35). Activation of β-catenin signaling in Wnt-10b–

transgenic skin, and in explanted fibroblasts, was associated with a substantial reduction in PPARγ levels. Moreover, Wnt-10b dramatically reduced 3T3-L1 preadipocyte differentiation into adipocytes in response to PPARγ ligands in vitro. In normal fibroblasts, ectopic Wnt-10b induced collagen gene expression. Reduced PPARγ expression and loss of subcutaneous adipose tissue in transgenic mice were associated with dermal fibrosis. Taken together, these observations suggest that ectopic Wnt-10b suppressed the adipogenic programs and concomitantly stimulated fibrogenic programs in cutaneous mesenchymal cells, directly contributing to excessive collagen deposition and fibrosis.

Although Wnt signaling is essential for normal embryonic development, in adults, aberrant Wnt expression, regulation, or activity is implicated in cancer, aging, and a variety of chronic diseases (12–14). Recent evidence from both animal models of fibrosis and human disorders links aberrant Wnt ligand expression or unregulated Wnt activity attributable to, for example, loss of endogenous inhibitors, with pathologic tissue remodeling and fibrosis. Aging-associated fibrosis of muscle can be attributed to up-regulated Wnt signaling (36). Transgenic mice with a stabilized mutant form of β-catenin that resists ubiquitin-mediated degradation ($Catnb^{lox[ex3]}$) showed exuberant wound healing and increased collagen synthesis (37). Genes associated with tissue remodeling such as plasminogen activator inhibitor 1, CTGF, and fibronectin are known Wnt/β-catenin transcription targets, although the mechanism of their regulation by Wnt remains ill-defined (38–41). It has been shown that CTGF induces mesenchymal stem cell differentiation into fibroblasts, and selective CTGF expression in fibroblasts results in tissue fibrosis in vivo (42,43).

Patients with idiopathic pulmonary fibrosis (IPF) have increased nuclear β-catenin in the lung (15). Moreover, fibrotic foci showed increased expression of Wnt-induced signaling protein 1 (WISP-1; a Wnt target gene) and low-density lipoprotein receptor–related protein 6 and glycogen synthase kinase 3β phosphorylation indicative of activated Wnt signaling at fibroblastic foci (44,45). Genome-wide transcriptional profiling of the lungs of patients with IPF revealed elevated expression of Wnt ligands, Wnt receptors, Wnt regulators, and Wnt targets such as osteopontin and WISP-1 (45,46), and explanted IPF fibroblasts maintained enhanced β-catenin activity (41). Importantly, inhibition of Wnt/β-catenin/CREB binding protein signaling reverses bleomycin-induced pulmonary fibrosis (47). We detected elevated β-catenin levels in fibrotic lungs from all 3 SSc patients with advanced lung disease who were examined (48). Beta-catenin was prominent in epithelial and fibroblastic cells in fibrotic foci. Several Wnt ligands are abnormally expressed in the TSK-1 mouse, and aberrant Wnt expression preceded the appearance of fibrosis (20). We also detected elevated *axin2* mRNA levels in a mouse model of scleroderma.

Interrogating microarray data sets generated from expression profiling of SSc skin biopsy specimens revealed increased mRNA levels of Wnt receptors (e.g., *Fzd2*) and Wnt target genes (e.g., *CCND*, *ASPM*), accompanied by reduced expression of the Wnt inhibitors *Wif1* and *Dkk2* (20,49, and Wei J, et al: unpublished observations). Dysregulated Wnt signaling is therefore associated with pathologic tissue remodeling in the skin and lungs and is implicated in the excessive matrix accumulation and myofibroblast differentiation that underlie fibrosis in SSc.

In summary, the results of the current study demonstrate that FABP4-driven ectopic Wnt-10b expression in transgenic mice drives β-catenin signaling in the skin associated with marked loss of subcutaneous adipose tissue, PPARγ expression, and adipogenesis, accompanied by reciprocal dermal fibrosis and TGFβ-independent up-regulation of markers of fibrogenesis. The mechanistic basis for the observed scleroderma phenotype in Wnt-10b–transgenic mice is likely to involve direct induction of fibrogenic transcription programs, possibly via induction of fibrogenic cytokines including CTGF, but remains to be fully elucidated. In light of the potent inhibitory effects of Wnt-10b on PPARγ expression and activity, our results suggest that excessive Wnt-10b/β-catenin signaling suppresses PPARγ-driven adipogenesis while promoting reciprocal fibrogenesis. Canonical Wnt signaling might therefore be an important novel antifibrotic target in SSc and related fibrosing conditions.

ACKNOWLEDGMENTS

We thank Tong-Chuan He (University of Chicago) for Wnt-10b adenovirus and members of the Varga laboratory for helpful discussions.

AUTHOR CONTRIBUTIONS

All authors were involved in drafting the article or revising it critically for important intellectual content, and all authors approved the final version to be published. Dr. Varga had full access to all of the data in the study and takes responsibility for the integrity of the data and the accuracy of the data analysis.

Study conception and design. Wei, Melichian, Gottardi, MacDougald, Varga.

Acquisition of data. Wei, Melichian, Komura, Hinchcliff.

Analysis and interpretation of data. Wei, Melichian, Lam, Lafyatis, Gottardi, MacDougald, Varga.

REFERENCES

1. Varga J, Abraham D. Systemic sclerosis: a prototypic multisystem fibrotic disorder. J Clin Invest 2007;117:557–67.
2. Denton CP, Black CM, Abraham DJ. Mechanisms and consequences of fibrosis in systemic sclerosis. Nat Clin Pract Rheumatol 2006;2:134–44.
3. Krieg T, Abraham D, Lafyatis R. Fibrosis in connective tissue disease: the role of the myofibroblast and fibroblast-epithelial cell interactions. Arthritis Res Ther 2007;9 Suppl 2:S4.
4. Postlethwaite AE, Shigemitsu H, Kanangat S. Cellular origins of fibroblasts: possible implications for organ fibrosis in systemic sclerosis. Curr Opin Rheumatol 2004;16:733–8.
5. Varga J, Pasche B. Transforming growth factor β as a therapeutic target in systemic sclerosis. Nat Rev Rheumatol 2009;5:200–6.
6. Rosenbloom J, Castro SV, Jimenez SA. Narrative review: fibrotic diseases: cellular and molecular mechanisms and novel therapies. Ann Intern Med 2010;152:159–66.
7. Van Amerongen R, Nusse R. Towards an integrated view of Wnt signaling in development. Development 2009;136:3205–14.
8. Cadigan KM, Liu YI. Wnt signaling: complexity at the surface. J Cell Sci 2006;119:395–402.
9. Willert K, Jones KA. Wnt signaling: is the party in the nucleus? Genes Dev 2006;20:1394–404.
10. Klapholz-Brown Z, Walmsley GG, Nusse YM, Nusse R, Brown PO. Transcriptional program induced by Wnt protein in human fibroblasts suggests mechanisms for cell cooperativity in defining tissue microenvironments. PLoS One 2007;2:e945.
11. Ohtola J, Myers J, Akhtar-Zaidi B, Zuzindlak D, Sandesara P, Yeh K, et al. β-catenin has sequential roles in the survival and specification of ventral dermis. Development 2008;135:2321–9.
12. Chien AJ, Moon RT. WNTS and WNT receptors as therapeutic tools and targets in human disease processes. Front Biosci 2007; 12:448–57.
13. Chien AJ, Conrad WH, Moon RT. A Wnt survival guide: from flies to human disease. J Invest Dermatol 2009;129:1614–27.
14. MacDonald BT, Tamai K, He X. Wnt/β-catenin signaling: components, mechanisms, and diseases. Dev Cell 2009;17:9–26.
15. Chilosi M, Poletti V, Zamo A, Lestani M, Montagna L, Piccoli P, et al. Aberrant Wnt/β-catenin pathway activation in idiopathic pulmonary fibrosis. Am J Pathol 2003;162:1495–502.
16. Selman M, Pardo A, Kaminski N. Idiopathic pulmonary fibrosis: aberrant recapitulation of developmental programs? PLoS Med 2008;5:e62.
17. Longo KA, Wright WS, Kang S, Gerin I, Chiang SH, Lucas PC, et al. Wnt10b inhibits development of white and brown adipose tissues. J Biol Chem 2004;279:35503–9.
18. Bennett CN, Longo KA, Wright WS, Suva LJ, Lane TF, Hankenson KD, et al. Regulation of osteoblastogenesis and bone mass by Wnt10b. Proc Natl Acad Sci U S A 2005;102:3324–9.
19. Bayle J, Fitch J, Jacobsen K, Kumar R, Lafyatis R, Lemaire R. Increased expression of Wnt2 and SFRP4 in Tsk mouse skin: role of Wnt signaling in altered dermal fibrillin deposition and systemic sclerosis. J Invest Dermatol 2008;128:871–81.
20. Lemaire R, Farina G, Bayle J, Dimarzio M, Pendergrass SA, Milano A, et al. Antagonistic effect of the matricellular signaling protein CCN3 on TGF-β- and Wnt-mediated fibrillinogenesis in systemic sclerosis and Marfan syndrome [published erratum appears in J Invest Dermatol 2010;130:2517]. J Invest Dermatol 2010;130:1514–23.
21. Wu M, Melichian DS, Chang E, Warner-Blankenship M, Ghosh AK, Varga J. Rosiglitazone abrogates bleomycin-induced scleroderma and blocks profibrotic responses through peroxisome proliferator-activated receptor-γ. Am J Pathol 2009;174:519–33.
22. Nadiri A, Kuchler-Bopp S, Haikel Y, Lesot H. Immunolocalization of BMP-2/-4, FGF-4, and WNT10b in the developing mouse first lower molar. J Histochem Cytochem 2004;52:103–12.
23. Lakos G, Takagawa S, Chen SJ, Ferreira AM, Han G, Masuda K, et al. Targeted disruption of TGF-β/Smad3 signaling modulates skin fibrosis in a mouse model of scleroderma. Am J Pathol 2004;165:203–17.
24. Takagawa S, Lakos G, Mori Y, Yamamoto T, Nishioka K, Varga J. Sustained activation of fibroblast transforming growth factor-β/Smad signaling in a murine model of scleroderma. J Invest Dermatol 2003;121:41–50.
25. Bhattacharyya S, Wei J, Melichian DS, Milbrandt J, Takehara K, Varga J. The transcriptional cofactor nab2 is induced by TGF-β and suppresses fibroblast activation: physiological roles and impaired expression in scleroderma. PLoS One 2009;4:e7620.
26. Hausman GJ. Techniques for studying adipocytes. Stain Technol 1981;56:149–54.
27. Ramirez-Zacarias JL, Castro-Munozledo F, Kuri-Harcuch W. Quantitation of adipose conversion and triglycerides by staining intracytoplasmic lipids with oil red O. Histochemistry 1992;97: 493–7.
28. Chen SJ, Yuan W, Mori Y, Levenson A, Trojanowska M, Varga J. Stimulation of type I collagen transcription in human skin fibroblasts by TGF-β: involvement of Smad 3. J Invest Dermatol 1999;112:49–57.
29. Ghosh AK, Bhattacharyya S, Lakos G, Chen SJ, Mori Y, Varga J. Disruption of transforming growth factor β signaling and profibrotic responses in normal skin fibroblasts by peroxisome proliferator–activated receptor γ. Arthritis Rheum 2004;50: 1305–18.
30. Gottardi CJ, Gumbiner BM. Role for ICAT in β-catenin-dependent nuclear signaling and cadherin functions. Am J Physiol Cell Physiol 2004;286:C747–56.
31. Wu M, Varga J. In perspective: murine models of scleroderma. Curr Rheumatol Rep 2008;10:173–82.
32. Martinez-Ferrer M, Afshar-Sherif AR, Uwamariya C, de Crombrugghe B, Davidson JM, Bhowmick NA. Dermal transforming growth factor-β responsiveness mediates wound contraction and epithelial closure. Am J Pathol 2010;176:98–107.
33. Wei J, Bhattacharyya S, Varga J. Peroxisome proliferator-activated receptor γ: innate protection from excessive fibrogenesis and potential therapeutic target in systemic sclerosis. Curr Opin Rheumatol 2010;22:671–6.
34. Wei J, Ghosh AK, Sargent JL, Komura K, Wu M, Huang QQ, et al. PPARγ downregulation by TGFβ in fibroblast and impaired expression and function in systemic sclerosis: a novel mechanism for progressive fibrogenesis. PLoS One 5:e13778.
35. Prestwich TC, Macdougald OA. Wnt/β-catenin signaling in adipogenesis and metabolism. Curr Opin Cell Biol 2007;19:612–7.
36. Brack AS, Conboy MJ, Roy S, Lee M, Kuo CJ, Keller C, et al. Increased Wnt signaling during aging alters muscle stem cell fate and increases fibrosis. Science 2007;317:807–10.
37. Cheon SS, Cheah AY, Turley S, Nadesan P, Poon R, Clevers H, et al. β-catenin stabilization dysregulates mesenchymal cell proliferation, motility, and invasiveness and causes aggressive fibromatosis and hyperplastic cutaneous wounds. Proc Natl Acad Sci U S A 2002;99:6973–8.
38. Chang W, Wei K, Jacobs SS, Upadhyay D, Weill D, Rosen GD. SPARC suppresses apoptosis of idiopathic pulmonary fibrosis fibroblasts through constitutive activation of β-catenin. J Biol Chem 2010;285:8196–206.
39. Chen S, McLean S, Carter DE, Leask A. The gene expression profile induced by Wnt 3a in NIH 3T3 fibroblasts. J Cell Commun Signal 2007;1:175–83.
40. Gustafson B, Smith U. Activation of canonical wingless-type MMTV integration site family (Wnt) signaling in mature adipocytes increases β-catenin levels and leads to cell dedifferentiation and insulin resistance. J Biol Chem 2010;285:14031–41.

41. He W, Tan R, Dai C, Li Y, Wang D, Hao S, et al. Plasminogen activator inhibitor-1 is a transcriptional target of the canonical pathway of Wnt/β-catenin signaling. J Biol Chem 2010;285: 24665–75.
42. Lee CH, Shah B, Moioli EK, Mao JJ. CTGF directs fibroblast differentiation from human mesenchymal stem/stromal cells and defines connective tissue healing in a rodent injury model. J Clin Invest 2010;120:3340–9.
43. Sonnylal S, Shi-wen X, Leoni P, Naff K, Van Pelt CS, Nakamura H, et al. Selective expression of connective tissue growth factor in fibroblasts in vivo promotes systemic tissue fibrosis. Arthritis Rheum 2010;62:1523–32.
44. Konigshoff M, Balsara N, Pfaff EM, Kramer M, Chrobak I, Seeger W, et al. Functional Wnt signaling is increased in idiopathic pulmonary fibrosis. PLoS One 2008;3:e2142.
45. Konigshoff M, Kramer M, Balsara N, Wilhelm J, Amarie OV, Jahn A, et al. WNT1-inducible signaling protein-1 mediates pulmonary fibrosis in mice and is upregulated in humans with idiopathic pulmonary fibrosis. J Clin Invest 2009;119:772–87.
46. Selman M, Pardo A, Barrera L, Estrada A, Watson SR, Wilson K, et al. Gene expression profiles distinguish idiopathic pulmonary fibrosis from hypersensitivity pneumonitis. Am J Respir Crit Care Med 2006;173:188–98.
47. Henderson WR Jr, Chi EY, Ye X, Nguyen C, Tien YT, Zhou B, et al. Inhibition of Wnt/β-catenin/CREB binding protein (CBP) signaling reverses pulmonary fibrosis. Proc Natl Acad Sci U S A 2010;107:14309–14.
48. Lam AP, Flozak AS, Russell S, Wei J, Jain M, Mutlu GM, et al. Nuclear β-catenin is increased in SSc pulmonary fibrosis and promotes lung fibroblast migration and proliferation. Am J Respir Cell Mol Biol 2011. E-pub ahead of print.
49. Whitfield ML, Finlay DR, Murray JI, Troyanskaya OG, Chi JT, Pergamenschikov A, et al. Systemic and cell type-specific gene expression patterns in scleroderma skin. Proc Natl Acad Sci U S A 2003;100:12319–24.